i-SAIRAS 2024

RoboGrav – Towards Force Sensitive Space Manipulators

Henry Maurenbrecher[1*], Maximilian Mühlbauer[3,1], Maxime Chalon[1,2], Alexander Kolb[1], Thomas Bahls[1], Bastian Deutschmann[1], Oxana Domsch[1], Markus Grebenstein[1,4], Maximilian Maier[1,2], Maximo A. Roa[1,2], Anton Shu[1], Thomas Sherevan[5], and Alin Albu-Schäffer[1,2,3]

*lead presenter, henry.maurenbrecher@dlr.de

[1] German Aerospace Center (DLR), Institute of Robotics and Mechatronics, Münchener Str. 20, 82234 Wessling, Germany

[2] KINETIK Space GmbH, Claude-Dornier-Str. 401, 82234 Weßling, Germany

[3] School of Computation, Information and Technology, Sensor Based Robotic Systems and Intelligent Assistance Systems, Technical University of Munich,
Friedrich-Ludwig-Bauer-Str. 3, Garching, Germany

[4] Monash University, Melbourne, Victoria, Australia

[5] iBOSS GmbH, Dennewartstr. 25-27, 52068 Aachen, Germany

Abstract—This paper introduces RoboGrav, a mission focused on the testing of a fully torque sensorized robotic arm under zero gravity conditions performed during the 42nd DLR parabolic flight campaign. Conducted in collaboration with the German Aerospace Center (DLR), KINETIK Space, iBOSS, the Technical University of Munich (TUM), and Novespace, RoboGrav aims to advance the development and testing of torque-controlled robotic manipulators for On-Orbit-Servicing (OOS) and space assembly tasks. The paper highlights the significant role of torque sensing, enhancing manipulation tasks under zero gravity conditions. Experimental tests were performed to ensure controller stability during free-space motions in zero gravity, using a pin shaped end effector for environmental interactions. External force sensing was employed to assess the robot's accuracy and performance across various controllers. This also enabled a comparison of the robot's behavior in both zero gravity and full-gravity environments, providing valuable insights into the transfer of Earth-developed algorithms to space applications. A simulated satellite docking task, using the iBOSS "iSSi" interface, demonstrated the robot's capability to manage position inaccuracies through impedance control, thus improving operational robustness. Technology developed for this project, such as the integration of torque sensors, the presented FPGA-based joint control algorithms and communication interfaces, high-level controllers and decision-making algorithms, can be transferred to future space missions. RoboGrav's torque-sensorized robotic arm offers valuable lessons and methodologies for future space servicing and space assembly missions.

Figure 1 RoboGrav system executing a mission during the parabolic flight

I. Introduction

A. State of the Art

The landscape of robotic space manipulation has evolved significantly, with notable contributions from systems such as the Shuttle Remote Manipulator System (SRMS) [1], and the Space Station Remote Manipulator System (SSRMS) [2]. The SRMS was a pioneering robotic system used on the Space Shuttle Missions to perform complex manipulation tasks, including satellite deployment and repairs. SRMS's success paved the way for its successor, SSRMS, enhancing capabilities including the integration of force-torque sensors [2], and working until today onboard the International Space Station (ISS). DLR pioneered the way for In-space Servicing, Assembly and Manufacturing (ISAM) applications starting in 1994 with the first robot in space controlled by VR technologies [3], and in the joint mission ETS-VII for teleoperating a robotic arm from JAXA [4]. DLR's ROKVISS mission [5] -the first torque controlled robotic system in space- demonstrated manipulation using force feedback teleoperation in the challenging space environment. In 2021, GITAI's S1 robotic arm successfully demonstrated autonomous and teleoperated execution of standard Intra-Vehicular Activity (IVA) tasks such as soft object manipulation and switch actuation onboard the ISS [6]. In 2023, GITAI demonstrated the S2, a dual arm autonomous robotic system, outside the ISS focusing on ISAM-specific tasks like fastening screws and thermal blanket manipulation [6]. Transitioning to terrestrial advancements, the torque controlled Lightweight Robot 3 (LWR3) [7] from DLR marked a significant leap forward in robotics. Its lightweight design and control systems laid down the foundation for versatile and cooperative robotic systems. This technology forms the basis of the development of the CAESAR arm [8] for space applications. Additionally, DLR developed the TINA arm [9], which demonstrated its versatility and adaptability in a study for a Mars Sample Return scenario [10]. DLR's RoboGrav Mission aims to validate the TINA arm technology under zero gravity, combining industry-proven technology and space-tested experience from ROKVISS, MASCOT [11] and the locomotion subsystem of the MMX Rover IDEFIX [12]. The validation of the electrical and mechanical designs for this can been classically performed with environmental testing using thermal vacuum chambers and vibration testing. However, the validation of the controller performance and operability can only be partially verified on ground. In particular, the effect of gravity on the structures maintains the joints in a loaded state, and power consumption is significantly higher, since the arm needs to lift itself. Compensation mechanisms like the MSS [13] still introduce unwanted disturbances, thus limiting the representativity of the testing. Only a limited set of options are available to test mechanisms under zero gravity. Drop towers and Sounding rockets are affordable, however they only offer a very limited duration of zero gravity. Parabolic flights, although more expensive, offer the major advantage that human operators can directly supervise the experiment, and if necessary, apply corrections. Finally, an ISS experiment offers the best duration, but involves additional constraints (flammability, toxicity, human safety issues) and carry a significant price tag. Hence, it was decided to validate the TINA system via a parabolic flight.

B. Mission

The RoboGrav experiment was conducted using the Novespace Air Zero G Airbus A310 as part of DLR's 42nd parabolic flight campaign. Over the course of three days, a total of 93 parabolas were flown, each providing approximately 22 seconds of near-zero gravity conditions (0 g $\pm 2 \cdot 10^{-2}$ g) [14]. Although brief, these zero-gravity periods were sufficient to conduct feature demonstrations of the robotic arm, divided into small, incremental tests with

holding phases in between. A key structural challenge was the exposure of the system to hyper gravity during the parabolic trajectory. The primary mission objective was to test various controllers in zero gravity. The features demonstrated during the experiments are:

- Simple free-path motion, as expected in inspection mission
- Soft interaction for maintenance and repair tasks
- Hard contact for docking activities.

These tests will help refining the system design and functionality in preparation for future space missions.

II. Device under Test

A. System Design

The mission's objective is to demonstrate the arm's potential for performing inspection, maintenance, and assembly tasks in zero gravity. To closely mimic the complex motions required in such applications and provide a realistic validation of the arm's capabilities, a four-degree-of-freedom (DoF) arm based on TINA joints was selected. While the 4-DoF configuration allows access to all points within the workspace, it limits the possible orientations of the end effector. In line with the RoboGrav mission profile, the automotive grade version of the TINA joints can be used. This approach offers a scalable foundation for future upgrades, where the system can be adapted for space flight requirements by replacing the components with space-qualified parts.

B. Mechanics

The mechanical design of the arm is based on the TINA arm, but using only four joints. The kinematics selected fort the RoboGrav mission is presented in Figure 2. There are two housings, each integrating one roll and one pitch axis together with their corresponding joint controller electronics. The robot has a length of 1257 mm, including the ball tip end effector. The arm joints use the S-sized version of the TINA arm actuators with 80 Nm nominal torque. The actuators are built around a Permanent Magnet Synchronous Motor, a Harmonic Drive gearbox and a torque sensor. The link side position is measured using a resolver. For the parabolic flights, the joints are equipped with brakes to support the robot weight during the hyper gravity phases. Due to security reasons the motors are turned off during the hyper gravity accelerations. The most noticeable difference to the previous TINA design is the redesigned housings. Indeed, one challenge during the assembly of previous TINA arms was the cabling of the circuit boards and the joints. In many cases, the bending radius of the cables could not be respected and, more importantly, the overall accessibility was poor, impairing inspection. In the new housing, presented in Figure 3, the control PCBs are

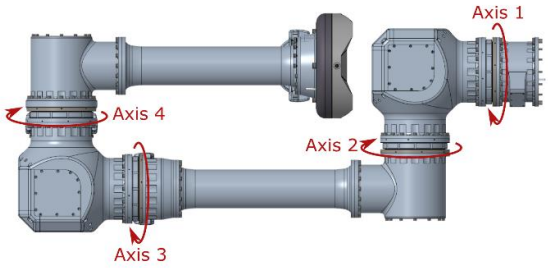

Figure 2 Kinematics of the RoboGrav system

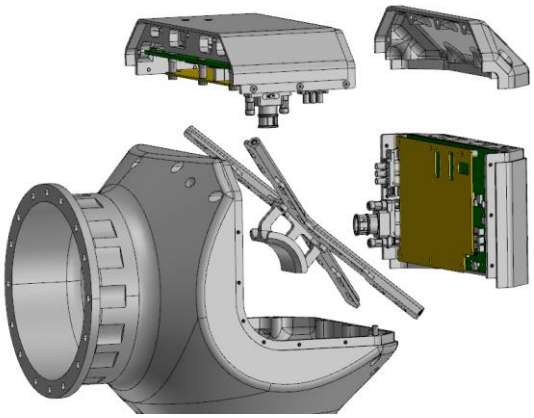

Figure 3 New housing design for RoboGrav

mounted on the opposing side to their respective joint and are fixed to the housing lids. This allows for a better accessibility and visibility during assembly as well as improving the thermal contact of the motor controller. The end of the arm was endowed with the iSSi (intelligent Space System Interface) interface, from iBOSS GmbH, which enables mechanical coupling, power, heat, and data transfer for modular satellite systems. This smart interface integrates an optical data transfer system, mechanical coupling elements and a highly conductive thermal interface made of a carbon nanotube copper-alloy composite. The interface is actuated by a brushless DC motor, provides a robust, rotatable, and redundant connection tested under extreme temperatures.

C. Electronics

The electronics architecture of the RoboGrav mission is centered around the use of SpaceWire as the primary fieldbus for controlling the robotic arm, similar to the TINA arm [9], [10]. An abstracted view of the overall communication architecture is shown in Figure 4. The mission is controlled by the Xiphos Q8 Onboard Computer (OBC), which plays a crucial role in managing the system's operations. The OBC is responsible for controlling the power supplies to the arm and controlling the robotic arm via the SpaceWire bus. Additionally, it handles communication with the application computer through an Ethernet connection, ensuring data transfer and mission control. The joint control PCB is based on the motor controller developed for MASCOT's mobility system [15]. It is centered around a flash-based FPGA. Power conditioning for the sensors and communication is realized on the board. Each PCB is dedicated to a single torque-controlled joint and includes: power conditioning, power inverter, Hall sensor decoding, resolver interface, torque sensor interface, SpaceWire physical layer, as well as the programming/debugging interface. Although it would be advantageous to use one power distribution system per shoulder in terms of volume and efficiency, experience gained with the TINA arm showed that independent controllers significantly reduce the integration and maintenance effort. The firmware for the RoboGrav mission is utilizing DLR's vendor independent SpaceWire core. The motor controller firmware uses a Hall sensor-based Space Vector Modulation (SVM) and a Torque Sensor Interface. It supports multiple operational modes:

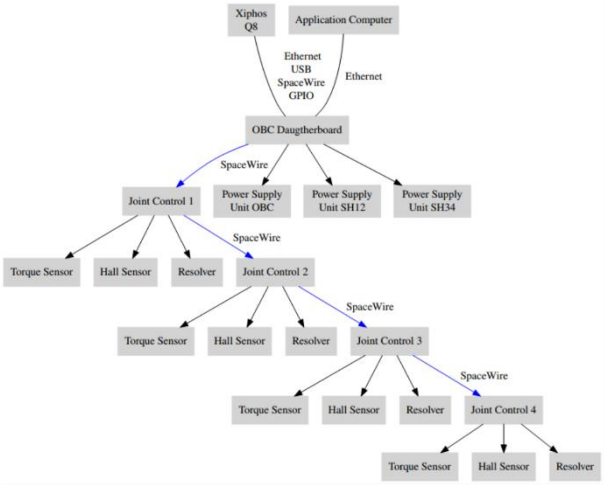

Figure 4 RoboGrav's digital interface architecture

- Stepper Mode: Directly controls the space vector for precise motor movements.
- Torque Control Mode: Utilizes torque sensors at the joints to regulate torque output.
- Position Control Mode: Employs Hall sensors at the joints for accurate position control.
- Cascaded Position and Torque Control Mode: Combines position and torque control to regulate the impedance of the joint, providing a versatile and adaptive control mechanism.

D. Software

The software of the RoboGrav mission is derived from the software originally developed for the SpaceDREAM mission [16]. Using the open source middleware ”links and nodes” allowed to connect an application computer via Ethernet and use this network connection to communicate with the OBC. The software is split accordingly into the real-time data processing for the robot, implemented on the OBC, and a high-level mission software coordinating the mission and parametrizing the controller on the application computer. On the OBC, a hardware abstraction layer (HAL) manages communication with the robot’s electronics via SpaceWire. It receives, validates and bundles the telemetry messages coming from each joint and then publishes them as telemetry information via ”links and nodes”. Incoming commands from the real-time controller are validated and then split into individual SpaceWire commands for each joint. Commands arriving too late at the joint will be ignored. In this case an internal watchdog triggers an error and enables the brakes of the robot. The real-time controller is based on a Simulink model for which C code is generated and cross-compiled using an automated toolchain [16]. Based on a joint pose interpolator and a state machine, joint space trajectories are computed and then sent to the low-level controllers, e.g. the position and impedance controllers implemented inside the robot’s joints. Also, adaptive virtual fixtures [17] are integrated in the Simulink model to allow for an easier teleoperation of the robotic arm. In addition a switch to enable and disable gravity compensation during the campaign was integrated. This is required to move the arm for changing the tools on ground and be able to move the robot during the steady flight phase with 1g acceleration. Also, a deadman button was directly integrated into the Simulink model. Releasing the deadman button immediately deactivates the robot and engages the brakes. The high-level mission software includes a base class from which individual mission scripts derive from. This implements interpolated point-to-point motions using different low-level controllers as well as parametrizing virtual fixtures. As the length of parabolas is not perfectly predetermined and the robot motion is controlled by the human operator using the deadman button, every operation can be interrupted at any time and will be resumed from the current robot’s pose. The mission script first moves the robot to a predetermined start pose during the steady flight phase with gravity compensation enabled and records the motion. Afterwards, the recording for the mission itself is started. While each mission is designed for a set of five parabolas, the mission will automatically restart after it is done. This minimizes workload for the operator, as the operator only has to start one mission script for a set of parabolas and stop it afterwards.

III. Testing

To achieve the goal of validating the 4-DoF robotic arm by executing selected feature demos utilizing its different control modes, the testing was structured to align with the parabolic flight schedule separating the goals of each day in the following:

- Day 1: Accuracy and applied forces
- Day 2: Docking with the iSSi interface and large movements
- Day 3: Hard interaction with the environment

Each experiment was conducted across multiple parabolas, with demonstrations performed during 22 s zero gravity intervals activated by the operator using the deadman button. On three experiment days, two different hardware setups were used for the experiments. For testing interactions of the arm with its environment, a pin end-effector was designed and several test objects with which interaction is possible were placed within the arm’s reach. This setup is

depicted in Figure 5, and was used to perform free-space motions (Sect. III-A), interaction with the spring with known rate and with different controllers (Sect. III-B), as well as experiments with virtual fixtures [17]. The second setup using the iBOSS ”iSSi” docking interface as end effector is depicted in Figure 6. This setup was used to perform more extensive motions using the full space available inside the rack (Sect. III-A) as well as to test docking maneuvers using different controllers (Sect. III-C).

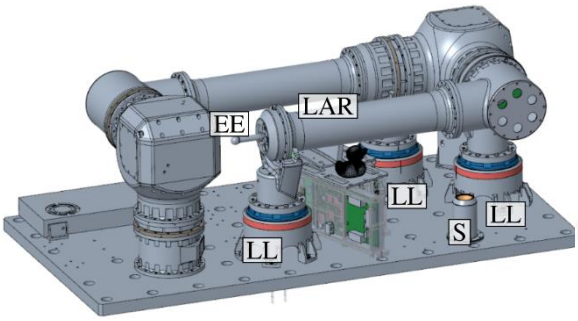

*Figure 5 RoboGrav's setup with pin as end effector **EE**, the spring assembly **S**, the launch adapter ring segment **LAR** (behind the robot arm), three launch locks **LL** on which the robot rests during start and landing*

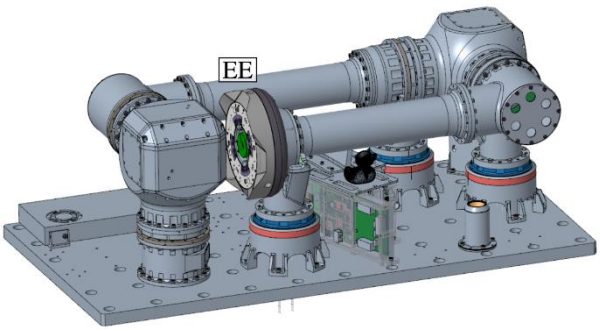

*Figure 6 RoboGrav's setup with iBOSS ”iSSi” docking interface as end effector **EE** . This is the only difference with respect to the setup in Figure 5.*

A. Joint-level and Cartesian Control

The joint controllers of the robot allow for position as well as impedance control, while the Simulink model running on the OBC adds an overlaid Cartesian impedance controller using a joint-level torque controller, computing joint torques to $\boldsymbol{\tau} = \mathbf{J}^{\mathrm{T}}\,\boldsymbol{\omega}$ from the Cartesian wrench $\boldsymbol{\omega}$. As a 4-DoF robot cannot achieve arbitrary poses inside its workspace, we only used this control law for the position part, omitting control of the orientation, which leads to a 1-dimensional nullspace of the robot that was controlled in ”elbow up” position. Trajectories obtained using those different controllers are depicted in Figures 7 to 9. Figure 7 shows the results of using a joint-level position controller under both 0g and 1g conditions. As the position controller only has a proportional factor and does not take gravity into account, the trajectories differ significantly with increasing distance of the end effector from the robot base. Under 0g, the robot end effector follows the given trajectory more closely (average offset: 1.5 cm) than under 1g (average offset: 1.8 cm. Especially in the most stretched position with $x \approx -0.7$ m where a large gravitational force needs to be compensated, the offset along the z axis gets bigger under 1g. The maximal offset along the z axis reaches 3.9 cm for the 1g case while under 0g, only 2.4 cm of offset is observed. In Figure 8,

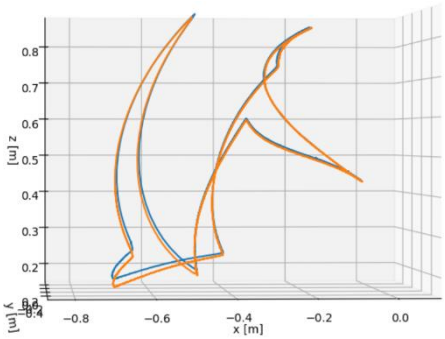

*Figure 7 End effector trajectory for extensive movements in **joint position control**. The blue trajectory was recorded during flight while the orange trajectory was recorded on ground.*

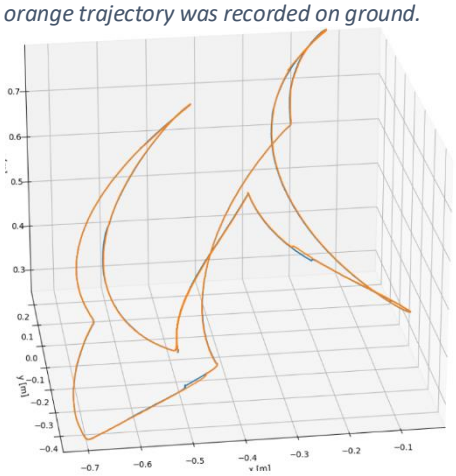

*Figure 8 End effector trajectory for extensive movements in **joint impedance control**. The blue trajectory was recorded during flight while the orange trajectory was recorded on ground.*

the same movements are executed using the joint-level impedance controller, which also takes gravity into account. This leads to smaller position errors even though the joint stiffness is set to a relatively small value of 1119 Nm/rad. Under 1g conditions, an average and maximum offset of 1.0 cm and 1.8 cm respectively are observed, while the 0g case gives very similar values with 1.0 cm and 1.8 cm. For the results using a Cartesian impedance control displayed in Figure 9 with a very high stiffness of 6000 Nm^{-1}-which is only possible because of the high internal damping of the robot- much higher accuracies can be achieved. Under 1g conditions, an average and maximum offset of 2.1 mm and10.7 mm respectively is observed, while the 0g case gives very similar values with 2.9 mm and 8.4 mm.

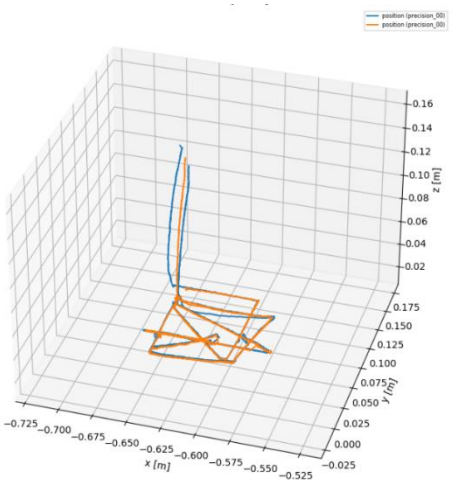

Figure 9 End effector trajectory for the "precision" experiment, where the robot's pin follows a Cartesian trajectory in the xy plane using Cartesian impedance control. The blue trajectory has been recorded during flight in zero gravity while the orange trajectory was recorded on ground.

B. Torque Measurement Validation

To validate the joint torque sensors, a spring with known rate and external dial gauge measuring the spring deflection was mounted to the base plate of the assembly (Figure 10). For a force of 30 N as measured by the external gauge, we measure joint torques of −0.8227 Nm, 15.2717 Nm, 5.0830 Nm, 0.1794 Nm for joints 1-4 under 0g conditions. This comes close to the expected values of −0.7182 Nm, 14.2477 Nm, 14.2477 Nm, 0.7144 Nm and shows that we can measure and control forces exerted on the environment.

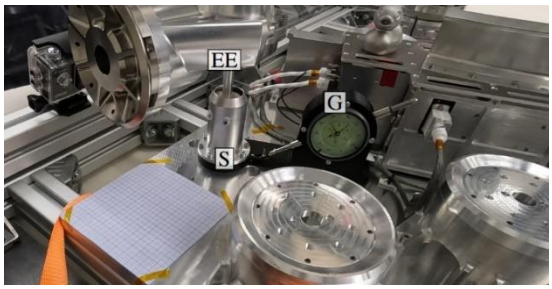

*Figure 10 End effector **EE** pressing the spring **S** with deflection measured using an external dial gauge **G.***

C. Docking of a Rigid Interface

In On-Orbit Servicing, docking to the target satellite is a critical operation. Given the inertias at play, the use of a position-controlled arm commonly results in excessive interface loads in case of misalignments. The availability of a torque sensor in the joints allows not only to monitor the interaction efforts, but to directly control them as part as the control loop. The impedance control, as implemented in our robot, allows to robustly handle positioning errors an guarantee that interface efforts adapted to the structural capabilities. Combined with an error tolerant interfaces like the iSSi adapter the system can cope with large deviation while handling the structures gently. This experiment focuses on the scenario of docking using both joint level

*Figure 11 Successful impedance-controlled docking of the end effector **EE** with mounted docking interface with the counterpart **I** mounted on the rack.*

and Cartesian impedance control, as shown in Figure 11. For the joint-level impedance control, the commanded docking position was perturbed to test that the docking manoeuvre still works with offsets which might e.g. come from errors in the perception system. Over six docking procedures, the error was gradually increased to a final offset 1.4 cm, which still allowed to achieve a successful docking. The robot was thus able to successfully compensate the maximum errors in weightlessness as well as in Earth's gravity.

IV. Conclusion

This paper described the RoboGrav mission, executed during DLR's 42nd Parabolic flight campaign, that demonstrated the use of a torque controlled robotic arm for in-orbit servicing operation. The mission demonstrated that the performance of the robot under 0g is at least as good if not better than under 1g. The findings confirm that developing and demonstrating on orbit servicing operation in the laboratory is a valid approach to the initial validation of space operation. The rich mixture of test cases and test configuration allows to verify a wide range of interaction, covering most of the expected use cases. In particular, the use of the iBOSS "iSSi" interface showed the robustness of the docking operation. Further, similar test campaigns, will be beneficial in order to validate new interaction questions, such as, for example, the contact dynamics while grasping a launch adapted ring on a light target.

References

[1] E. Wu, J. Hwang, and J. Chladek, "Fault-tolerant joint development for the Space Shuttle Remote Manipulator System: Analysis and experiment," IEEE Trans. on Robotics and Automation, vol. 9, no. 5, pp.675–684, 1993.

[2] R. McGregor and L. Oshinowo, "Flight 6a: deployment and checkout of the space station remote manipulator system (SSRMS)," in Proc. Int. Symp. on Artificial Intelligence, Robotics and Automation in Space (iSAIRAS), 2001.

[3] G. Hirzinger, "ROTEX - the first robot in space controlled by VR based technologies," in Virtual World Research & Development, Realta Virtuale Expo (Virtual Reality Expo), 1994.

[4] K. Landzettel, B. Brunner, K. Deutrich, G. Hirzinger, G. Schreiber, and B. Steinmetz, "DLR's experiments on the ETS VII space robot mission," in Proc. IEEE Int. Conf. Advanced Robotics (ICAR), 1999.

[5] G. Hirzinger, K. Landzettel, D. Reintsema, C. Preusche, A. Albu Schäffer, B. Rebele, and M. Turk, "ROKVISS – robotics component verification on ISS," in Proc. Int. Symp. on Artifical Intelligence,Robotics and Automation in Space (iSAIRAS), 2005.

[6] M. Johnston, A. Smith, and S. Williams, "In-space servicing, assembly, and manufacturing (ISAM) state of play," NASA, Tech. Rep.,2023, accessed: 2024-08-09. [Online]. Available: https://www.nasa.gov/wp-content/uploads/2023/10/isam-state-of-play-2023.pdf

[7] G. Hirzinger, N. Sporer, A. Albu-Schäffer, M. Hähnle, R. Krenn, A. Pascucci, and M. Schedl, "DLR's torque-controlled light weight robot III - are we reaching the technological limits now?" in Proc. IEEE Int. Conf. Robotics and Automation (ICRA), 2002, pp. 1710–1716.

[8] A. Beyer, G. Grunwald, M. Heumos, M. Schedl, R. Bayer, W. Bertleff, B. Brunner, R. Burger, J. Butterfaß, R. Gruber, T. Gumpert, F. Hacker, E. Kramer, M. Maier, S. Moser, J. Reill, M. A. Roa, H.-J. Sedlmayr, ¨N. Seitz, M. Stelzer, A. Stemmer, G. Tubio Manteiga, T. Wimmer, M. Grebenstein, C. Ott, and A. Albu-Schäffer, "Caesar: Space robotics ¨technology for assembly, maintenance, and repair," in Proc. Int. Astronautical Congress (IAC), 2018.

[9] M. Maier, M. Chalon, M. Pfanne, R. Bayer, M. M. Mascarenhas, H.-J. Sedlmayr, and A. L. Shu, "TINA: Small torque controlled robotic arm for exploration and small satellites," in Proc. Int. Astronautical Congress (IAC), 2019.

[10] M. Maier, T. Bahls, R. Baver, M. Bihler, M. Chalon, W. Friedl, N. Höger, C. Hofmann, A. Kolb, A. M. Sundaram, M. Pfanne, H.-J. Sedlmayr, and N. Seitz, "TINA: The modular torque controlled robotic arm - a study for Mars Sample Return," in Proc. IEEE Aerospace Conf., 2021, pp.1–10.

[11] J. Reill, H.-J. Sedlmayr, P. Neugebauer, M. Maier, E. Krämer, and ¨R. Lichtenheldt, "MASCOT - asteroid lander with innovative mobility mechanism," in Proc. ESA Symp. on Advanced Space Technologies for Robotics and Automation (ASTRA), 2015.

[12] J. Bertrand, S. Tardivel, F. IJpelaan, E. Remetean, A. Torres, S. Mary, M. Chalon, F. Buse, T. Obermeier, M. Smisek, A. Wedler, J. Reill, and M. Grebenstein, "Roving on phobos: Challenges of the MMX rover for space robotics," in Proc. ESA Symp. on Advanced Space Technologies in Robotics and Automation (ASTRA), 2019.

[13] F. Elhardt, R. Boumann, M. De Stefano, R. Heidel, P. Lemmen, M. Heumos, C. Jeziorek, M. A. Roa, M. Schedl, and T. Bruckmann,"The motion suspension system – MSS: A cable-driven system for on ground tests of space robots," in Advances in Mechanism and Machine Science, M. Okada, Ed. Springer, 2023, pp. 379–388.

[14] Novespace, "Novespace flight info," 2024, https://www.airzerog.com/science-faq/ [Accessed: 04. September 2024].

[15] M. Maier, M. Chalon, J. Reill, and H.-J. Sedlmayr, "Highly integrated, radiation-hardened, motor controller with phase current measurement, "in Proc. ESA Symp. on Advanced Space Technologies for Robotics and Automation (ASTRA), 2017.

[16] M. Muhlbauer, M. Chalon, M. Ulmer, and A. Albu-Schäffer, "Software for the SpaceDREAM robotic arm" 2024 [Online] Available: https://arxiv.org/abs/2409.17562

[17] M. Muhlbauer, T. Hulin, B. Weber, S. Calinon, F. Stulp, A. Albu- Schäffer, and J. Silverio, "A probabilistic approach to multi-modal ´adaptive virtual fixtures," IEEE Robotics and Automation Letters, vol. 9,no. 6, pp. 5298–5305, 2024.